PAPER

High-temperature creep properties of NIFS-HEAT-2 high-purity low-activation vanadium alloy

IOP Publishing | International Atomic Energy Agency Nuclear Fusion

Nucl. Fusion **59** (2019) 096046 (6pp) https://doi.org/10.1088/1741-4326/ab1c8f

High-temperature creep properties of NIFS-HEAT-2 high-purity low-activation vanadium alloy

T. Nagasaka[1], T. Muroga[1], T. Tanaka[1], A. Sagara[1], K. Fukumoto[2], P.F. Zheng[3] and R.J. Kurtz[4]

[1] National Institute for Fusion Science, Toki, Japan
[2] Research Institute of Nuclear Engineering, University of Fukui, Tsuruga, Japan
[3] Southwestern Institute of Physics, Chengdu, China
[4] Pacific Northwest National Laboratory, Richland, WA, United States of America

E-mail: nagasaka@nifs.ac.jp

Received 7 January 2019, revised 19 March 2019
Accepted for publication 25 April 2019
Published 6 August 2019

Abstract

A low-activation vanadium alloy with the composition of V-4 mass% Cr-4 mass% Ti is an alternative to reduced activation ferritic/martensitic steels for blanket structural material in fusion reactors. The NIFS-HEAT-2 (NH2) is the world's highest-purity V–4Cr–4Ti alloy among over 30 kg scale heats. The processes to purify this heat have successfully enhanced workability, weldability and low-activation characteristics, however degradation of high-temperature strength was a concern due to possible purification softening. Therefore, the present study evaluated high-temperature creep properties of NH2 at around the operation temperature, 700 °C–800°C. The degradation of creep properties, such as shorter rupture time and enhanced creep rate, were observed for NH2, compared with a conventional US heat in the stress range of 150–200 MPa. On the other hand, it was revealed that these creep properties were comparable to those of the US heat in the lower applied stress of 100 MPa, though only short term rupture data are available at this moment. Since design stress for fusion blankets is expected below 100 MPa, purification up to the level of NH2 will induce no negative impact on the blanket service conditions.

Keywords: fusion reactor blanket, high temperature strength, interstitial impurity effect

1. Introduction

The National Institute for Fusion Science (NIFS) pursued scale-up of low-activation vanadium alloy production with a nominal composition of V-4 mass% Cr-4 mass% Ti, based on industrial-scale fabrication technologies, and developed the NIFS-HEAT-1 (NH1) and -2 (NH2) in collaboration with Japanese universities [1, 2]. Table 1 summarizes the chemical compositions of vanadium alloys in the world with the heat size of 30 kg or more. A US Department of Energy (DOE) program produced the largest 500 kg (US832665) and 1200 kg (US832864) heats before NIFS-HEATs [4, 8]. These pioneering heats enabled study on fabrication technologies for welding and tubing for vanadium alloys. However, the weld joint exhibited brittle fracture at room temperature, due to ductility loss caused by interstitial impurities, such as C, N and O, in the plate before welding [9]. In addition, these impurities were accumulated in the tubing process by pick up from the atmosphere during the intermediate annealing, and induced crack defects on the surface [10]. It is crucial to reduce these impurity levels in the as-melt alloy ingot and to minimize the impurity pick up during the breakdown process to final products. In order to purify the alloy products and improve the ductility further, a goal for NIFS-HEATs was set to reduce these harmful impurities to less than 100 mass ppm for each element. Since they originate mainly from the ingredient vanadium metal, it was purified by using high-purity Al as the reducing agent and Ar as the atmosphere in thermic reduction of raw vanadium pentoxide, V_2O_5. The improved process does not increase the cost significantly,

Table 1. Chemical compositions of low-activation alloys with the fabrication scale of 30 kg or more.

ID	Country	Fabrication size/kg	Alloying elements/mass%			Interstitial impurities/mass ppm			
			V	Cr	Ti	C	N	O	C + N + O
NIFS-HEAT-2 [3]	Japan	166	Bal.	4.02	3.98	69	122	148	339
US832665 [4]	USA	500	Bal.	3.25	4.05	170	100	330	600
RF-VVC3 [5]	Russia	110	Bal.	3.76	4.64	290	100	200	590
SWIP-30 [6]	China	30	Bal.	3.81	3.92	130	20	270	420
CEA-J57 [7]	France	30	Bal.	3.76	3.93	70	110	290	470
ID	Harmful high-activation impurities/mass ppm								
	Al	Co	Nb	Ni	Mo	Al + Co + Nb + Ni + Mo			
NIFS-HEAT-2	59	0.7	0.8	7	24	92			
US832665	355	0.295	60	9.6	315	740			
RF-VVC3	240		<10	<5	68	308			
SWIP-30	100			82	35	217			
CEA-J57	190	0.4	<10	17	75	282			

Chemical analysis method for NH2: Cr, Ti: ICP-OES, C: combustion infrared absorption, N: He carrier fusion thermal conductivity, O: He carrier fusion infrared absorption, Nb: ICP-MS, others: GD-MS [3].
US: C, N, O: not specified, others: GD-MS [4].
RF and SWIP: not specified [5, 6].
CEAJ-57: Cr, Ti: ICP-OES, Co, Ni, Mo: GD-MS, others: specified just as ICP [7].
Although the accuracy, such as the detection limit, depends on the method, element and the background condition at each analysis, it is typically 1 mass ppm for C, N, O, 10 mass ppm for metallic elements in ICP-OES and 0.1 mass ppm in ICP-MS and GD-MS analyses.

and is still suitable for industrial-scale production. The purified vanadium contained 40–90 mass ppm C, 60–160 mass ppm N and 40–100 mass ppm O, nearly satisfying the goals. Although some increase in O impurity is observed for NH2 compared with the above-mentioned level, the total of interstitial impurity level (C + N + O) of NH2 is almost half that of the US832665. As a result, weldabilty and workability were successfully improved because of enhanced ductility [4, 9, 11]. The new process also reduced metallic impurities creating long-lived radioactive isotopes, such as Al, Co, Nb, Ni and Mo. Figure 1 shows decay curves for the contact dose rate at the plasma facing surface of a blanket made of either NH2 or the US vanadium alloy after neutron irradiation with a wall loading of 2 MW m^{-2} for 5 years (100 dpa), assuming a neutron energy spectrum of a V-Li blanket in FFHR-2m1 reactor design with 35%-^{6}Li enrichment [12]. The curves were not calculated for the other alloys because the impurity concentrations for the critical elements, Co, Nb and Ni, have not determined yet by chemical analysis. NH2 satisfies the quasi-hands-on limit, 10^{-4} Sv h^{-1}, after 170 years of storage and cooling, where material recycling is possible with simple radiation shielding, such as about 5 cm thick lead, for workers. Although many properties were improved by the purification, possible degradation of high-temperature strength due to purification softening was a concern, because the impurities are hardening agents, and NH2 is the highest purity alloy as indicated by the total impurity levels, (C + N + O) and (Al + C o + Nb + Ni + Mo) in table 1. In tensile tests on NH2, slight degradation of yield strength has been observed at 750 °C and 800 °C, compared with the US alloy as shown in figure 2. In the high-temperature region, the thermal creep properties will determine the operating temperature limit of vanadium alloys,

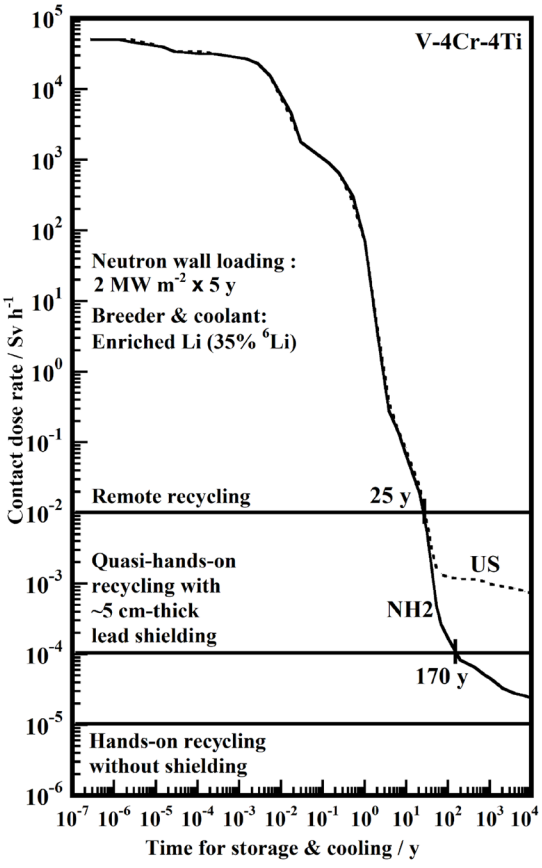

Figure 1. Decay curves for the contact dose rate at the plasma facing surface of a blanket made from NH2 or US vanadium alloy after neutron irradiation with wall loading of 2 MW m^{-2} for 5 years (100 dpa).

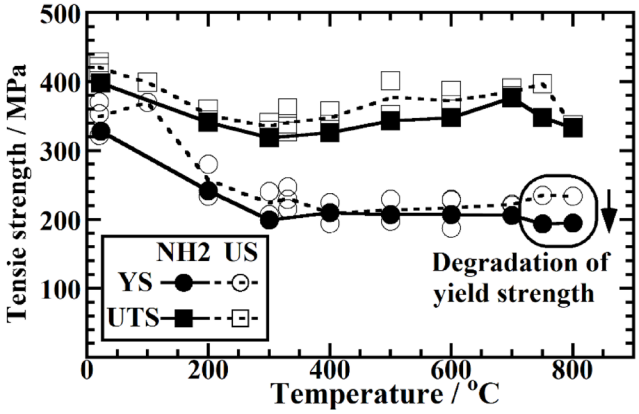

Figure 2. Comparison of yield strength (YS) and ultimate tensile strength (UTS) of NH2 and US832665 (US) in tensile tests. Data are transferred from [13, 14]. The final heat treatment was an annealing at 1000 °C for 2 h for both materials after cold rolling with a reduction of 98 and 40 % for NH2 and US, respectively.

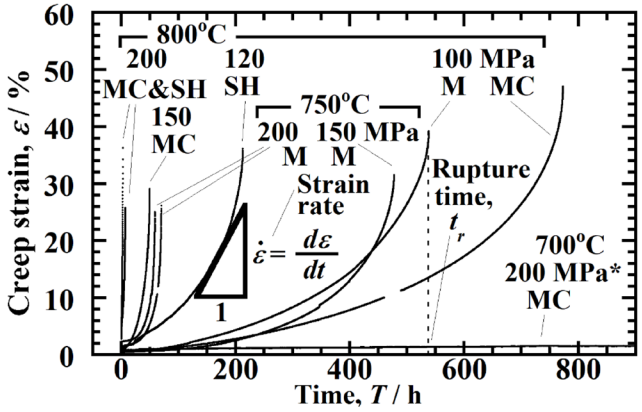

Figure 3. Time-strain creep curves. SH, MT, M and MC indicate the creep testing machines used, and are SHIMADZU AG-1kNXplus, INTESCO MT-100, M-100 and MC-100, respectively. *Test at 700 °C under 200 MPa was terminated at 2375 h before fracture.

and it is a potential concern if these properties are degraded. Therefore, the present study evaluated the high-temperature creep properties of NH2 and sought to determine the deformation mechanisms at elevated temperatures for a highly purified vanadium alloy.

2. Experimental procedure

Tensile-type specimens with gauge dimensions of 0.25 mm × 1.2 mm × 5 mm were punched out from a 0.25 mm thick sheet of 98%-cold-rolled NH2. The specimens were annealed for recrystallization at 1000 °C for 2 h. The average grain size after the final heat treatment is 18 μm. Creep tests were conducted in a mechanical test facility at NIFS with universal mechanical testing machines, SHIMADZU AG-1kNXplus, INTESCO MT-100 and M-100, and a dead-weight type creep testing machine, INTESCO MC 100, equipped with vacuum chambers. The vacuum during the creep tests was better than 10^{-4} Pa and was further degassed with Zr foil getter around the specimen. A contact strain gauge was not available in the present experiments, however displacement of specimen holders was measured with a linear variable differential transformer (LVDT) of type MHR250, TE Connectivity Co. for SHIMADZU AG-1kNXplus and type MHR500 for the others, with a resolution of 0.5 micron, which is equivalent to 0.01% strain. The specimen holders were connected to the LVDTs, using quartz rods. On-line measurement of creep strain by the LVDTs sometimes failed because of slide of the quartz rod in the specimen holders. In such cases, creep curves and creep rate could not be calculated, while rupture time data were obtained.

3. Results and discussion

Figure 3 shows creep strain versus time curves for the creep tests on NH2. Creep rupture time and creep rate were obtained from these curves. A creep test, for example, with an applied stress of 200 MPa at 700 °C was terminated at 2375 h due to a trip of the cooling system of the creep testing facility. In this case, creep rate was analysed from the creep curve before the termination and creep rupture time was estimated as more than the termination time. At this moment, creep data with smaller applied stress than the tensile yield stress, which is about 200 MPa in the test temperature range as shown in figure 2, are available only at 750 °C and 800 °C, because creep tests with lower stress and at lower temperatures take much time and are currently ongoing. Creep tests under 150 and 200 MPa at 800 °C and 200 MPa at 750 °C were repeated twice. One of the rupture times was different from the other one by a factor of about three. In other words, data scatter for the rupture time was ±50% based on the average value. Figure 4 plots the stress dependence of the creep rupture time, comparing NH2 data with the US alloy [15]. The NH2 data for 800 °C in the lower applied stress region was comparable to the US heat, although in the higher stress region, the creep rupture time was shorter than the dashed trend line for US data. The data for 200 MPa and 700 °C is plotted and shown by an asterisk, though the test was terminated before the fracture. This data proved that the rupture time was no less than the termination time, 2375 h, and was comparable to that for the US alloy. The other data for 700 °C creep with larger applied stress indicated shorter rupture time than the US alloy. While comparable rupture time data at low applied stresses has not been obtained for 750 °C yet, the data for NH2 at 200 MPa also shows considerable deviation from the dashed trend lines for US data. In conclusion, creep rupture time for NH2 at relatively higher stress region was shorter, compared with the US alloy.

Figure 5 shows the minimum creep rate. Consistent with the above rupture data, the minimum creep rate of NH2 is likely greater than that of the US heat in the higher stress region. A general formula for steady state creep is as follows,

$$\dot{\varepsilon} = \frac{A\sigma^m}{d^n} \mathrm{e}^{-\frac{Q}{RT}}, \quad (1)$$

where $\dot{\varepsilon}$ is the minimum creep rate, A is a constant, σ is applied stress, m is the stress exponent, d is grain size, n is the grain size exponent, Q is the creep activation energy, R is the gas

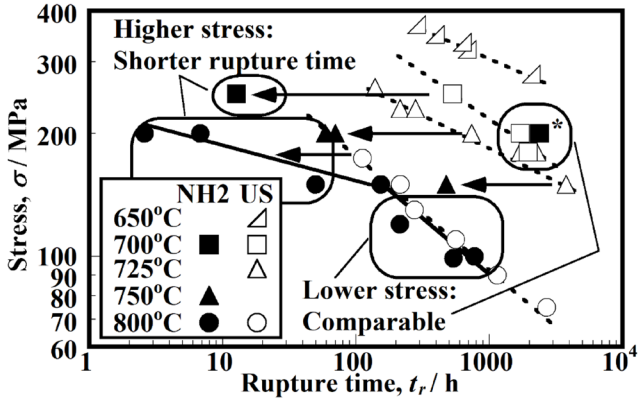

Figure 4. Creep rupture stress versus rupture time. Data for the US alloy were transferred from [15]

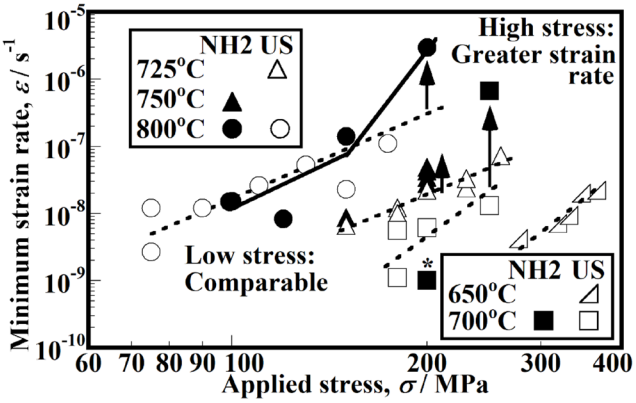

Figure 5. Stress dependence of the minimum creep strain rate.

constant, and T is test temperature. In the present study, d is 18 μm and constant in the test temperature range. The logarithm of equation (1) is

$$\ln \dot{\varepsilon} = \ln \frac{A\sigma^m}{d^n} - \frac{Q}{RT}. \quad (2)$$

Under constant applied stress, σ,

$$\ln \dot{\varepsilon} = A_0 - \frac{Q}{RT}, \quad (3)$$

where A_0 is again constant and the slope in Arrhenius-type plots for the minimum creep rate give the creep activation energy, Q. In order to discuss creep mechanisms, Q was estimated based on equation (3) with data set of the minimum creep rate, ε_i, for different test temperatures, T_i, under the constant applied stress condition,

$$Q = \left(R \ln \frac{\varepsilon_1}{\varepsilon_2}\right) / \left(\frac{1}{T_1} - \frac{1}{T_2}\right). \quad (4)$$

Figure 6 presents the Arrhenius plots for the minimum creep rate. Figure 7 plots the creep activation energy, which is the slope of the lines in figure 6. Since the scattering of the rupture time is 50% based on the average value, similar uncertainty is expected for the creep rate and can be converted into 150 kJ mol^{-1} in error for the estimation of creep activation energy. Assuming the US data also contains similar uncertainties,

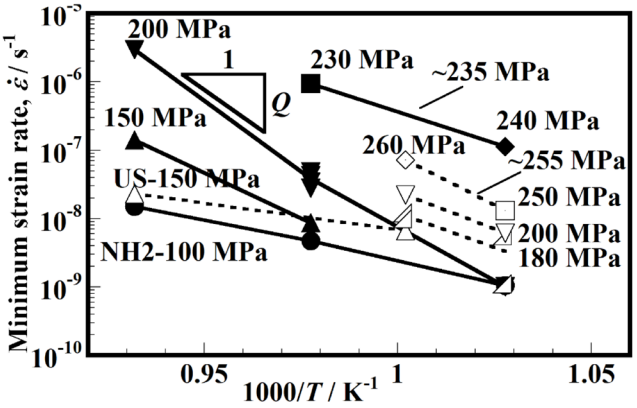

Figure 6. Arrhenius plots for the minimum creep strain rate. Solid and dashed lines indicate the data for NH2 and US, respectively. Data for NH2 with 100 and 235 MPa, and all for US were calculated based on the creep rates in [15, 16], respectively.

error bars of 150 kJ mol^{-1} are indicated in figure 7. The creep activation energy of the US heat is 320 kJ mol^{-1} in average over the stress range of 150–200 MPa, and is close to the activation energy for self-diffusion in pure vanadium, 300 kJ mol^{-1} [17], within the uncertainties. Self-diffusion can enhance the climbing motion of dislocations, and in addition, the stress range is relatively high and approaches the yield stress, around 200 MPa, shown in figure 2. Therefore, climb-assisted dislocation motion is thought to be preferable compared with the other diffusional creep, such as grain boundary creep, and is considered as the predominant process for creep in this regime. NH2 showed similar activation energy at 100 MPa, however an activation energy higher than 500 kJ mol^{-1} at 150 MPa and above. Considering that the activation energy at 235 MPa is again about the same level as the US alloys, these analyses may include much error, probably because the creep rate was calculated from only one or two creep curves at each temperature. In addition, thermal activation process with such high activation energy is hardly attributed to, for example, activation energy for diffusion of the alloying elements in vanadium matrix, Ti and Cr, which are similar to the self-diffusion energy of vanadium, 285 [18] and 270 [19] kJ mol^{-1}, respectively. The analyses indicate that the creep activation energy was consistent with the self-diffusion of vanadium and the climbing assisted creep mechanism in the low stress region for NH2 at 100 MPa and for the US alloy at 150 to 200 MPa.

In order to explain the enhanced creep at high stress and the deterioration of creep rupture time, it is necessary to consider an additional deformation mechanism activated by the purification for NH2. According to tensile data shown in figure 2, the YS of NH2 was comparable to the US heat at around 700 °C, however it was smaller than that of the US heat at 750 °C and 800 °C. Hardening by dynamic strain aging (DSA) due to a Cottrell atmosphere of interstitial impurities has been observed for V–4Cr–4Ti [20]. Interstitial impurities can form Cottrell atmospheres on dislocations, pinning them, and requiring additional stress to unpin prior to yielding by dislocation glide. The present creep test temperature range, 700 °C to 800 °C, is around the boundary for disappearance of DSA due to thermal

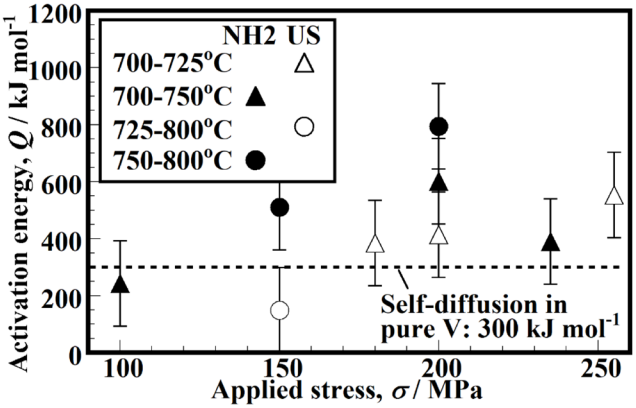

Figure 7. Apparent activation energy for creep. Data for NH2 with 100 and 235 MPa, and all for US were calculated based on the creep rates in [15, 16], respectively.

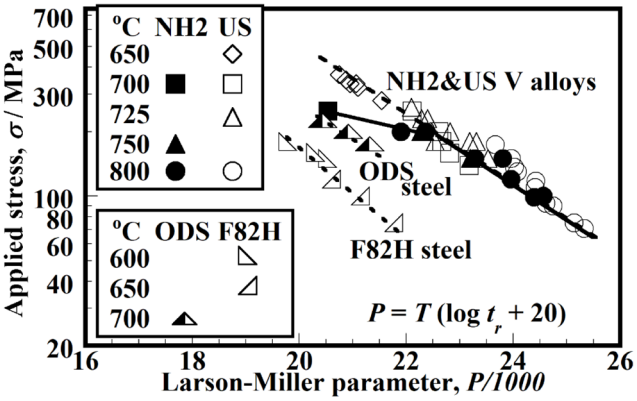

Figure 8. Larson–Miller plot for NH2, US heat [15, 21], F82H steel [22] and 9Cr-ODS steel [23]. High σ and high P draw high creep strength and long creep life at high temperature.

de-trapping of interstitial impurities [20]. Lower levels of interstitial impurities probably resulted in less effective dislocation pinning by enhanced thermal de-trapping at 750 °C and 800 °C, and lead to a lower YS for NH2. Since the applied stress in the creep tests, 150 to 200 MPa, was close to the YS of NH2, dislocation glide without climbing is a possible mechanism for the additional deformation process, and could be activated by the enhanced de-trapping of interstitial impurities due to the purification. In the lower stress region, the dislocation climb mechanism is predominant and not affected by interstitial impurities, because the dislocation motion in climbing is much slower than in gliding, so that the atmosphere could follow the dislocation motion without any unpinning.

The creep data were converted by time-temperature equivalence scaling using the Larson–Miller parameter as shown in figure 8. The parameters for NH2 with larger applied stress than 200 MPa are smaller than those for the US heat, however are still comparable to the US data in the low stress region and superior to fusion-grade F82H ferritic steel and 9Cr oxide-dispersion-strengthened (9Cr-ODS) steel. As mentioned above, creep properties were not degraded by the purification at stress levels around 100 MPa. The allowable design stress would be no more than one-quarter UTS, about 80 MPa, in the case of V–4Cr–4Ti alloy, if the allowable design stress is determined with the typical design code for nuclear structural materials [24]. It is concluded that use of high-purity V–4Cr–4Ti, such as NH2, requires no change in the blanket design stress, though creep is enhanced due to purification softening in the higher stress region.

4. Conclusions

No degradation of creep properties was observed for the high-purity low-activation vanadium alloy NIFS-HEAT-2 at stress levels below 100 MPa, compared with a conventional vanadium alloy, US832665. At higher stress levels, a reduction in rupture time and an increase in creep rate were observed in NIFS-HEAT-2. Lower yield stress of NIFS-HEAT-2 suggests an additional deformation process, which might be dislocation glide activated by thermal de-trapping of interstitial impurities due to the purification. The purification for NIFS-HEAT-2 improved many properties, such as weldability, workability and low-activation characteristics, and raised no negative effect on high-temperature creep properties under projected blanket service stresses.

Acknowledgments

This work was conducted under the framework of Fusion Engineering Research Project in National Institute for Fusion Science, and supported by budget code UFFF023. RJK support provided by the U.S. Department of Energy, Office of Fusion Energy Sciences under Contract DE-AC05-76RL01830.

References

[1] Muroga T. and Nagasaka T. 2000 Development of manufacturing technology for high purity low activation vanadium alloys *Proc. 18th IAEA Fusion Energy Conf. (Sorrento, Italy, 4–10 October 2000)* FTP1/09 (www.iaea.org/inis/collection/NCLCollectionStore/_Public/33/028/33028871.pdf)

[2] Nagasaka T., Muroga T., Fukumoto K.-I., Watanabe H., Grossbeck M.L. and Chen J.M. 2006 Development of fabrication technology for low activation vanadium alloys as fusion blanket structural materials *Nucl. Fusion* **46** 618–25

[3] Nagasaka T., Muroga T., Wu Y.C., Xu Z.G. and Imamura M. 2002 Low activation characteristics of several heats of V–4Cr–4Ti ingot *J. Plasma Fusion Res. Ser.* **5** 545–50

[4] Grossbeck M.L., Klueh R.L., Cheng E.T., Peterson J.R., Woolery M.R. and Bloom E.E. 1998 Analysis of V–Cr–Ti alloys in terms of activation of impurities *J. Nucl. Mater.* **258–63** 1778–83

[5] Potapenko M.M., Chernov V.M. and Drobyshev V.A. 2009 Large heats V-4Ti-4Cr alloys and items for fusion power reactors *14th Intl. Conf. Fusion Rector Materials (Sapporo, Japan, 6–11 September 2009)*

[6] Fu H.Y., Chen J.M., Zheng P.F., Nagasaka T., Muroga T., Li Z.D., Cui S. and Xu Z.Y. 2013 Fabrication using electron beam melting of a V–4Cr–4Ti alloy and its

thermo-mechanical strengthening study *J. Nucl. Mater.* **442** S336–40
[7] Duquesnes V., Guilbert T. and Flem M.L. 2012 French investigation of a new V–4Cr–4Ti grade: CEA-J57—fabrication and microstructure *J. Nucl. Mater.* **426** 96–101
[8] Johnson W.R. and Smith J.P. 1998 Fabrication of a 1200 kg ingot of V–4Cr–4Ti alloy for the DIII-D radiative divertor program *J. Nucl. Mater.* **258–63** 1425–30
[9] Nagasaka T., Grossbeck M.L., Muroga T. and King J.F. 2001 Comparison of impact property of Japanese and US reference heats of V–4Cr–4Ti after gas-tungsten-arc welding *Fusion Technol.* **39** 664–8
[10] Rowcliffe A.F., Hoelzer D.T., Johnson W.R. and Young C. 2003 Fabrication of creep tubing from the US and NIFS heats of V–4Cr–4Ti *Fusion Materials Semiannual Progress Report* DOE-ER-0313/35 pp 6–21
[11] Nagasaka T., Muroga T. and Iikubo T. 2003 Development of tubing technique for high-purity low activation vanadium alloys *Fusion Sci. Technol.* **44** 465–9
[12] Tanaka T., Muroga T. and Sagara A. 2005 Tritium self-sufficiency and neutron shielding performance of self-cooled liquid blanket system for helical reactor *Fusion Sci. Technol.* **47** 530–4
[13] Nagasaka T., Muroga T., Li M.M., Hoelzer D.T., Zinkle S.J., Grossbeck M.L. and Matsui H. 2006 Tensile property of low activation vanadium alloy after liquid lithium exposure *Fusion Eng. Des.* **81** 307–13
[14] Zinkle S.J., Rowcliffe A.F. and Stevens C.O. 1998 High temperature tensile properties of V–4Cr–4Ti *Fusion Materials Semiannual Progress Report* DOE/ER-0313/24 pp 11–4
[15] Natesan K., Soppet W.K. and Rink D.L. 2000 Uniaxial creep behaviour of V–4Cr–4Ti alloy *Fusion Materials Semiannual Progress Report* DOE/ER-0313/29 pp 37–40
[16] Zheng P.F., Nagasaka T., Muroga T., Chen J.M. and Li Y.F. 2011 Creep properties of V–4Cr–4Ti strengthened by cold working and aging *Fusion Eng. Des.* **86** 2561–4
[17] Peart R.F. 1965 Diffusion of V^{48} and Fe^{59} in vanadium *J. Phys. Chem. Solids* **26** 1853–61
[18] Pelleg J. 1978 Diffusion in niobium and vanadium *Rev. High-Temp. Mater.* **4** 5–45
[19] Japan Institute Metals (ed) 1984 *Metal Data Book in Japanese* 2nd edn (Tokyo: Maruzen)
[20] Miyazawa T., Nagasaka T., Hishinuma Y., Muroga T., Li Y.F., Satoh Y., Kim S.W. and Abe H. 2013 Effect of yttrium on dynamic strain aging of vanadium alloys *J. Nucl. Mater.* **442** S341–5
[21] Kurtz R.J., Ermi A.M. and Matsui H. 2001 An update on biaxial thermal creep of vanadium alloys *Fusion Materials Semiannual Progress Report* DOE-ER-0313/31 pp 7–16
[22] Shiba K., Hishinuma A., Tohyama A. and Masamura K. 1997 *JAERI-Tech 97-038* Japan Atomic Energy Research Institute
[23] Muroga T., Nagasaka T., Li Y.F., Abe H., Ukai S., Kimura A. and Okuda T. 2014 Fabrication and characterization of reference 9Cr and 12Cr-ODS low activation ferritic/martensitic steels *Fusion Eng. Des.* **89** 1717–22
[24] 2015 *ASME Boiler & Pressure Vessel Code* 3rd edn (New York: ASME)